

**EFFECT OF INDIUM ADDITION ON
MICROSTRUCTURE, WETTABILITY, SHEAR
STRENGTH AND CREEP BEHAVIOR OF SN100C
SOLDER**

NABIHAH BINTI ABDULLAH

UNIVERSITI SAINS MALAYSIA

2019

**EFFECT OF INDIUM ADDITION ON
MICROSTRUCTURE, WETTABILITY AND
CREEP BEHAVIOR OF SN100C SOLDER**

by

NABIHAH BINTI ABDULLAH

**Thesis submitted in fulfilment of the requirements
for the degree of
Master of Science**

February 2019

ACKNOWLEDGEMENT

First and foremost, I would like to express my deepest appreciation to Universiti Sains Malaysia, especially School of Materials and Mineral Resources Engineering for providing an appropriate and healthy environment as well as resources and necessary infrastructures to accomplish my project. My appreciation goes to the Dean of School of Materials and Mineral Resources Engineering, Professor Dr. Zuhailawati Binti Hussain for being considerable and thoughtful.

I would like to express my utmost gratitude to my helpful and respectful supervisor, Assoc. Prof. Dr. Nurulakmal Binti Mohd Sharif for the support, guidance and encouragements throughout the semester for me to complete my research project. Besides the expertise comments, constructive suggestion and regular followed up on my progress. I would also like to thank the Ministry of High Education Malaysia's Sponsorship (MyBrain15) for the financial support.

I take this opportunity to express gratitude to Nadirah, Fitriah and all the technical staff for providing me guidance and help in equipment utilization and giving me useful recommendations in solving problem for this research project. I am also immensely grateful to my beloved family for their continuous help and support. I also place on record, my sense of gratitude to all who directly or indirectly lent their helping hand in completing this research project.

TABLE OF CONTENTS

ACKNOWLEDGEMENT	ii
TABLE OF CONTENTS	iii
LIST OF TABLES	vi
LIST OF FIGURES	viii
LIST OF EQUATION	xii
LIST OF ABBREVIATIONS	xiii
LIST OF SYMBOLS	xvi
ABSTRAK	xix
ABSTRACT	xxi
CHAPTER 1 INTRODUCTION	1
1.1 Research Background	1
1.2 Problem Statement	3
1.3 Objective	4
1.4 Project Overview	5
CHAPTER 2 LITERATURE REVIEW	6
2.1 Introduction	6
2.2 Soldering Technique.....	8
2.2.1 Wave soldering	8
2.2.2 Reflow Soldering	9
2.2.3 Hand Soldering	11
2.3 Flux.....	12
2.4 Lead Free Solder	13
2.4.1 Binary Alloy.....	14
2.4.2 Ternary Alloys	18
2.4.3 Effect of Indium Addition on Sn Based Lead-Free Solder	20
2.5 Solder Characterization	22
2.5.1 Wettability (Spreading test)	22
2.5.2 Wettability Test (Wetting Balance Method).....	25
2.5.3 Thermal Properties	26
2.6 Lap Joint Test	27
2.7 Intermetallic Compound (IMC).....	28
2.8 Fundamentals of Creep.....	31
2.8.1 Quantitative Aspect of Creep.....	31
2.8.2 Temperature Dependence of Secondary Creep Rate	33

2.8.3	Stress Dependent of Secondary Creep Rate.....	35
2.8.4	Creep Mechanism	38
2.8.5	Creep Model of Solder Alloys	43
2.8.6	Creep Constant.....	45
CHAPTER 3 MATERIAL AND METHOD		47
3.1	Introduction	47
3.2	Raw material.....	47
3.2.1	Solder Alloys	47
3.2.2	Copper Substrate	49
3.2.3	Flux	49
3.3	Sample preparation.....	50
3.3.1	Solder preparation.....	50
3.3.2	Substrate Preparation	52
3.3.3	Reflow.....	53
3.4	Solder Characterization	54
3.4.1	X-Ray Fluorescent (XRF) Analysis.....	54
3.4.2	Differential Scanning Calorimetry (DSC) Analysis	55
3.4.3	Scanning Electron Microscopy (SEM) and Energy Dispersive X-Ray (EDX) Analysis.....	55
3.5	Wettability Evaluation.....	56
3.5.1	Spreading and Wetting Angle Evaluation.....	56
3.5.2	Wettability Balance Test.....	57
3.6	IMC Evaluation	58
3.7	Single Lap Joint Shear Test.....	59
3.8	Creep Test.....	61
CHAPTER 4 RESULT AND DISCUSSION		63
4.1	Introduction	63
4.2	X-ray Fluorescent (XRF) Analysis of Solder Alloys	63
4.3	Differential Scanning Calorimetry (DSC) Analysis.....	64
4.4	Microstructure of Bulk Solder.....	69
4.5	Wettability Evaluation.....	78
4.5.1	Spreading and Contact Angle Test	78
4.5.2	Wettability Balance Test.....	82
4.6	Intermetallic Compound Formation (IMC) Evaluation.....	87
4.6.1	SEM Image of Solder Joint.....	87
4.6.2	IMC Thickness.....	91
4.7	Single Lap Joint Shear Test.....	94

4.7.1	Fractography of Lap Joint Shear Test.....	97
4.8	Creep Test.....	100
4.8.1	Creep Curve	100
4.8.2	Creep Stress Exponent (n) Determination	103
4.8.3	Creep Activation Energy (Q) Determination.....	109
4.8.4	Fractography of Creep Test	113
CHAPTER 5 CONCLUSION AND RECOMMENDATION.....		118
5.1	Conclusion.....	118
5.2	Recommendations	120
REFERENCES.....		121
APPENDICES		
APPENDIX A: XRF DATA		
APPENDIX B: WETTING BALANCE TEST		
APPENDIX C: IMC THICKNESS MEASUREMENT		
APPENDIX D: EXAMPLE OF CALCULATION FOR POSSIBLE IMC PHASES		
APPENDIX E: EDX RESULTS FOR BULK MICROSTRUCTURE		
APPENDIX F: CREEP TEST		
LIST OF PUBLICATIONS		

LIST OF TABLES

		Page
Table 2.1	Wetting categories of solder alloys (Mayhew and Wicks, 1971).	23
Table 2.2	Variation of creep exponent and activation energy with stress and temperature(Evan and Wilshire, 1993).	45
Table 3.1	Chemical composition of solder alloy in wt.%	50
Table 3.2	List of dimensions of copper substrate according to the test requirement.	52
Table 4.1	Desired composition of solder alloys in wt.%	63
Table 4.2	XRF results for the composition of the solder alloys in wt.%	64
Table 4.3	DSC table for melting temperature, crystallization temperature onset melting temperature, onset crystallization temperature and the degree of undercooling.	67
Table 4.4	Example of weight percentage calculation.	77
Table 4.5	EDX result of bulk SN100C solder alloy with In addition.	77
Table 4.6	Wettability based on contact angle value (Mayhew and Wicks, 1971).78	78
Table 4.7	Wetting angle and spreading test of solder alloys.....	81
Table 4.8	Data derived from data of wetting graphs curve for SN100C solder after 6	84
Table 4.9	Data obtained from the wetting balance curve for the solder alloys....	85
Table 4.10	IMC particles and layer at interface of solder/Cu substrate with In addition.	91
Table 4.11	The average IMC thickness of solder alloys on Cu substrate.....	92
Table 4.12	Average shear strength of solder sample.	95
Table 4.13	Average shear strength of solder sample after aging 150°C for 100 hours.	96
Table 4.14	Shear modulus under different temperature.....	103
Table 4.15	Steady-state creep rate for all solder joint at different temperature and stresses.....	105
Table 4.16	The creep stress exponents of all solder joints at different test temperature.	108

Table 4.17	Creep activation energy of all solder joints.	112
------------	--	-----

LIST OF FIGURES

	Page
Figure 2.1	Evolution of electronic packaging technology(Tunga, 2008)..... 7
Figure 2.2	Schematic diagram of wave soldering process(Liukkonen et al., 2011). 9
Figure 2.3	Schematic diagram of reflow soldering process (Ressana,2016)..... 11
Figure 2.4	Schematic diagram of hand soldering process (Clear, 2011). 12
Figure 2.5	Sn-Cu phase diagram (Satyanarayan & Prabhu, 2011). 15
Figure 2.6	Phase diagram of Sn-Ag solder alloys..... 16
Figure 2.7	Phase diagram of Sn-In solder alloys (www.Himikatus.ru, 2017)..... 17
Figure 2.8	(a) Ternary phase diagram showing the Sn–Ag–Cu ternary eutectic reaction and (b) Calculated liquidus surface for Sn-Ag-Cu (Kattner & Boettinger, 1994) (cont.)..... 18
Figure 2.9	Ternary phase diagram showing the Sn-Cu-Zn ternary, and (b) Calculated liquidus surface for Sn-Cu-Zn (Ali et al., 2016)..... 20
Figure 2.10	Schematic diagram of wetting angle using Young-Dupre equation (Ayyad 2010). 23
Figure 2.11	Typical wetting curve in wetting balance technique (Satyanarayan & Prabhu, 2011)..... 25
Figure 2.12	DSC results during heating (endothermal) and cooling (exothermal) for (a) SAC (0507), (b) SAC (0507)–0.05Ni and (c) SAC (0507)–0.1Ni solder alloys (Hammad, 2013)..... 27
Figure 2.13	Various lap join configurations (Adhesivestoolkit, 2002)..... 28
Figure 2.14	Schematic diagram of the growth mechanism of Cu ₆ Sn ₅ at the Sn-Ag-Cu /Cu interface(Lee & Mohamad, 2013a)..... 29
Figure 2.15	(a) Schematic cross-section of a solder joint, and (b) SEM observation of the IMC layer(Tong An, 2013). 30
Figure 2.16	Schematic diagram creep testing(Jin et al., 2014) 31
Figure 2.17	Steady-state shear creep rate versus applied shear stress(Schubert et al., 2001) 32
Figure 2.18	The stress and temperature dependence of creep(Chiu et al., 2012). ... 33

Figure 2.19	The steady-state stress versus strain-rate at difference temperature(El-Daly & Hammad, 2012).....	35
Figure 2.20	Applied stress dependence on the steady-state creep strain rate for determination stress exponent (n) values at 25, 80 and 130 °C for Sn–5Sb, Sn–5Sb–3.5Ag and Sn–5Sb–1.5Au solder alloy(El-Daly et al., 2009).	37
Figure 2.21	Showing slip of an edge dislocation(Benaarbia et al., 2018).	39
Figure 2.22	Vacancy movement or self-diffusion (Cook et al., 2005).	40
Figure 2.23	Nabarro and Herring creep model (Michael et al., 2004).....	41
Figure 2.24	A model for the formation of cracks due to grain boundary sliding(Xie et al., 2017)	43
Figure 3.1	Flow of experimental works.	48
Figure 3.2	Heating profile for solder alloy.....	51
Figure 3.3	Dimension of specimen for spreading, wetting angle and reflow process.	53
Figure 3.4	Heating profile for reflow process.....	54
Figure 3.5	Diagram of the measurement of spreading area and wetting angle.....	57
Figure 3.6	Experimental setup for wettability curve test.	58
Figure 3.7	Schematic diagram of wetting balance test.	58
Figure 3.8	IMC thickness measurement of reflowed samples using software iSolution DT.	59
Figure 3.9	Dimension of specimen for shear test (dimensions are in mm).....	60
Figure 3.10	Experimental setup of lap joint shear test.....	61
Figure 3.11	Schematic diagram of Creep and Rupture Testing Machine.	62
Figure 3.12	Experimental setup of creep test.....	62
Figure 4.1	DSC curves during heating process SN100C, SN100C.0.5In, SN100C.1.0In, SN100C.1.0In, SN100C.1.5In and SN100C.2.0In. ...	65
Figure 4.2	DSC curves during cooling process SN100C, SN100C.0.5In, SN100C.1.0In, SN100C.1.0In, SN100C.1.5In and SN100C.2.0In. ...	66
Figure 4.3	SEM micrograph and EDX results of SN100C bulk solder alloy a) (500X) b) (3000X).....	71
Figure 4.4	SEM micrograph and EDX results of SN100C.0.5In bulk solder alloy a) (500X) b) (3000X).	72

Figure 4.5	SEM micrograph and EDX results of SN100C.1.0In bulk solder alloy a) (500X) b) (3000X).	73
Figure 4.6	SEM micrograph and EDX results of SN100C.1.5In bulk solder alloy a) (500X) b) (3000X).	74
Figure 4.7	SEM micrograph and EDX results of SN100C.2.0In bulk solder alloy a) (500X) b) (3000X).	75
Figure 4.8	Reflowed solder on Cu substrate for spreading test (a) SN100C, (b) SN100C.0.5In, (c) SN100C.1.0In, (d) SN100C.1.5In, (e) SN100C.2.0In	80
Figure 4.9	Spreading test of solder alloys	80
Figure 4.10	Reflowed solder on Cu substrate for wetting angle (a) SN100C, (b) SN100C.0.5In, (c) SN100C.1In, (d) SN100C.1.5In, (e) SN100C.2In.	81
Figure 4.11	Average wetting angle of solder alloys.	82
Figure 4.12	Illustrates data of wetting graphs curve for SN100C solder after six times test.	83
Figure 4.13	Wetting time of solder alloys.....	86
Figure 4.14	Maximum wetting force, F_{max} of solder alloy.	86
Figure 4.15	SEM micrographs of as-reflowed a)SN100C, b)SN100C.0.5In, c)SN100C.1.0In, d)SN100.1.5In, e)SN100C.2.0In (cont.).....	88
Figure 4.16	Schematic of interfacial of solder alloys/Cu during solder reflow (a) dissolution of the Cu substrate, (b) supersaturation of the molten solder layer with Cu, (c) formation of the scallop-type Cu_6Sn_5 at the interface and (d) Cu_3Sn emerges between Cu_6Sn_5 /Cu with prolonged soldering (Lee & Mohamad, 2013b).	90
Figure 4.17	Schematic diagram of IMC thickness measurement.	92
Figure 4.18	Average IMC thickness (μm).	93
Figure 4.19	Fracture path of sample show failure at solder joint area.....	95
Figure 4.20	Comparison of shear strength of lap joint between reflow and aging (150°C, 100 hours).....	97
Figure 4.21	Morphology of the fractographies of SN100C/Cu solder lap joint shear test (a) reflow and (b) after aging 150°C for 100 hours.....	98
Figure 4.22	Morphology of the fractographies of SN100C.0.5In/Cu solder lap joint shear test (a) reflow and (b) after aging 150°C for 100 hours.	98

Figure 4.23 Morphology of the fractographies of SN100C.1.0In/Cu solder lap joint shear test (a) reflow and (b) after aging 150°C for 100 hours.	99
Figure 4.24 Morphology of the fractographies of SN100C.1.5In/Cu solder lap joint shear test (a) reflow and (b) after aging 150°C for 100 hours.	99
Figure 4.25 Morphology of the fractographies of SN100C.2.0In/Cu solder lap joint shear test (a) reflow and (b) after aging 150°C for 100 hours.	99
Figure 4.26 Creep curves of SN100C at different testing temperatures.	101
Figure 4.27 Creep Curve of SN100C at different testing stress levels.	101
Figure 4.28 Comparison of creep curves for all solder joint.....	102
Figure 4.29 Steady-state shear creep rate versus applied shear stress (Schubert et al., 2001).	104
Figure 4.30 Creep curve with linear creep strain of SN100C.1.5In at stress 55MPa and temperature 116°C(389K).....	104
Figure 4.31 Creep stress exponent of SN100C solder joint.	106
Figure 4.32 Creep stress exponent of SN100C.0.5In solder joint.....	106
Figure 4.33 Creep stress exponent of SN100C.1.0In solder joint.....	106
Figure 4.34 Creep stress exponent of SN100C.1.5In solder joint.....	107
Figure 4.35 Creep stress exponent of SN100C.1.0In solder joint.....	107
Figure 4.36 Creep activation energy of SN100C solder joint.	110
Figure 4.37 Creep activation energy of SN100C.0.5In solder joint.	110
Figure 4.38 Creep activation energy of SN100C.1.0In solder joint.	111
Figure 4.39 Creep activation energy of SN100C.1.5In solder joint.	111
Figure 4.40 Creep activation energy of SN100C.2.0In solder joint.	111
Figure 4.41 Morphology of the creep fractography of SN100C-2.0In solder joint at stress of 55MPa and 116°C.....	114
Figure 4.42 Morphology of the creep fractography of SN100C-2.0In solder joint at stress of 55MPa and 185°C.....	115
Figure 4.43 Morphology of the creep fractography of SN100C-2.0In solder joint at stress of 77MPa and 116°C.....	116
Figure 4.44 Morphology of the creep fractography of SN100C-2.0In solder joint at stress of 77MPa and 185°C.....	117

LIST OF EQUATION

		Page
Equation 2.1	$\gamma_{SL} + \gamma_{LGC} \cos \theta - \gamma_{SG} = 0$	24
Equation 2.2	$\cos \Theta = \frac{\gamma_{SG} - \gamma_{SL}}{\gamma_{LG}}$	24
Equation 2.3	$\dot{\epsilon}_{ss} = A_2 \cdot \text{Exp.}^{-(QRT)}$	35
Equation 2.4	$\dot{\epsilon}_{ss} = A_1 \sigma^n$	37
Equation 2.5	$\dot{\epsilon}_{ss} = A_3 \exp(a\sigma)$	37
Equation 2.6	$\dot{\epsilon}_{ss} = A_4 \sinh(a\sigma)$	37
Equation 2.7	$\dot{\epsilon}_{ss} = u(\sigma) \cdot V(T)$	38
Equation 2.8	$\dot{\epsilon}_{ss} = A_5 \sigma^n \exp^{-(QRT)}$	38
Equation 2.9	$\dot{\epsilon} = A \frac{Gb}{RT} D \left(\frac{b}{d}\right) \left(\frac{\tau}{G}\right)^n$	44
Equation 2.10	$\dot{\epsilon} = A \frac{D_0 Gb}{RT} \left(\frac{b}{d}\right)^P \left(\frac{\tau}{G}\right)^n \exp\left(\frac{-Q}{RT}\right)$	45
Equation 2.11	$\dot{\epsilon} = A \left(\frac{\tau}{G}\right)^n \exp\left(-\frac{Q}{RT}\right)$	45
Equation 2.12	$n = \left[\frac{\partial \ln \dot{\epsilon}}{\partial \left(\frac{\tau}{G}\right)} \right]_T$	45
Equation 2.13	$Q = -R \left[\frac{\partial \ln \dot{\epsilon}}{\partial \left(\frac{1}{T}\right)} \right]_\tau$	45
Equation 3.1	Shear Strength (MPa) = $\frac{\text{Load (N)}}{\text{Area (m}^2\text{)}}$	60

LIST OF ABBREVIATIONS

ASTM	American Society for Testing and Material
Ag	Argentum (silver)
Al	Aluminium
Au	Gold
BGA	Ball Grid Array
Bi	Bismuth
Cd	Cadmium
Ce	Cerium
Co	Cobalt
cm	Centimeter
CNC	Computer Numerical Control
CSPs	Chip scale packages
Cu	Copper
DIP	Dual In Line Package
DSC	Differential Scanning Calorimetry
EDX	Electron Dispersive X-Ray Spectroscopy
Fe	Iron
g	Gram (weight)
Ga	Gallium
Ge	Germanium
IC	Integrated circuit

IMC	Intermetallic Compound
In	Indium
kN	Kilo Newton
mg	Milligram
min	Minute (time)
mm	Milimeter (length)
mol	Molecular
MPa	Mega Pascal
Ni	Nickel
μm	Micrometer
OM	Optical Microscopy
OSP	Organic solderability protection
P	Phosphorus
Pb	Plumbum
Pd	Palladium
Pt	Platinum
PTH	Pin Through Hole
PCB	Printed Circuit Board
PGA	Pin Grid Array
RA	Activated rosin
RoHS	Restriction of Hazardous Substance
S	Sulphur
SAC	Sn-Ag-Cu

SAL	Sebatian Antara Logam
Sb	Antimony
Sec	Second
SEM	Scanning Electron Microscopy
SMT	Surface Mount Technology
SN100C	Sn-0.7Cu-0.05Ni-Ge
SN100C-0.5In	Sn-0.7Cu-0.05Ni-0.5In
SN100C-1In	Sn-0.7Cu-0.05Ni-1In
SN100C-1.5In	Sn-0.7Cu-0.05Ni-1.5In
SN100C-2In	Sn-0.7Cu-0.05Ni-2In
Sn	Stanium (Tin)
SnCu	Copper-tin
SnIn	Indium-tin
SnPb	Lead-tin
SnZn	Zinc-tin
SnCuNi	Tin-Copper-Nickel
SnCuIn	Tin-Copper-Indium
SnAgCu	Tin-Silver-Copper
SnCuBi	Tin-Copper-Bismuth
XRF	X-Ray Fluorescent
Zn	Zinc

LIST OF SYMBOLS

A	Area
β -Sn	Sn-rich phase
$^{\circ}\text{C}$	Celsius
$^{\circ}\text{C}/\text{min}$	Degree Celsius per minute
d	IMC thickness after aging
d_0	Initial IMC thickness
D	Diffusion coefficient
D_0	Intrinsic Diffusivity
ϵ	Creep strain
$\dot{\epsilon}$	Creep strain rate
ϵ_0	Instantaneous Creep Strain
ϵ_{pc}	Primary Creep Strain
$\epsilon_{p\&s}$	Primary and Steady State Creep Strain
$\dot{\epsilon}_{ss}$	Steady State Creep Strain Rate
$^{\circ}\text{F}$	Fahrenheit (temperature)
F	Wetting force
F_b	Buoyancy force
F_e	End force
F_{max}	Maximum wetting force
F_w	Withdrawal force
G	Shear Modulus

J	Joule
m	meter
μ	micron
N	Newton
n	Creep Stress Exponent
η	Homologous Temperature
ρ	Density of the Solder
Q	Activation energy
R	Gas constant
S_b	Ratio of wetting force just before withdrawal to the wetting force during complete wetting
t_1	Wetting time
T	Temperature
T_c	Crystallization temperature
T_m	Melting temperature
τ	Shear Stress
θ	Wetting angle
θ_c	Contact Angle
σ	Stress
γ	Surface tension of solder
γ_{sg}	Surface tension between solid and gas
γ_{sl}	Surface tension between solid and liquid
γ_{lg}	Surface tension between liquid and gas

°C Degree Celsius

% Percentage

wt% Weight percent

**KESAN PENAMBAHAN INDIUM TERHADAP MIKROSTRUKTUR,
KEBOLEHBASAAN, KEKUATAN RICIH DAN KELAKUAN RAYAPAN
PATERI SN100C**

ABSTRAK

Disebabkan kebimbangan toksik plumbum terhadap alam sekitar, penggunaan pateri tanpa plumbum telah digunakan secara meluas dalam industri pembungkusan elektronik. Dalam mencari alternatif menggantikan pateri plumbum, pateri bebas plumbum haruslah mempunyai takat lebur yang hampir sama dengan pateri plumbum (183°C), serta mempunyai kebolehbasaan, sifat fizikal dan mekanikal yang baik. Diantara pateri bebas plumbum, aloi Sn-Cu pateri menunjukkan kesesuaian yang baik untuk menggantikan pateri plumbum. Walau bagaimanapun, pateri Sn-Cu pateri mempunyai takat lebur dan sudut basahan yang tinggi berbanding dengan pateri plumbum. Takat lebur yang tinggi akan menyebabkan suhu pematerian tinggi yang membawa risiko lebih tinggi terhadap komponen dan substrat yang sensitif dan tidak dapat menahan suhu tinggi. Tujuan projek ini adalah untuk mengkaji tingkah laku haba, mikrostruktur, kebolehbasaan, sifat mekanikal dan kelakuan rayapan SN100C pateri (Sn-0.7Cu-0.05Ni-0.01Ge) dengan penambahan indium (0.5,1.0,1.5 dan 2.0wt%). Ciri-ciri, mikrostruktur, sifat fizikal dan mekanikal dan kelakuan rayapan pateri SN100C telah dikaji menggunakan mikroskop optik, mikroskop imbasan elektron, kalorimeter imbasan perbezaan, dan mesin Instron. Dengan penambahan indium 0wt% ke 2.0wt%, suhu lebur menurun dari 229.64°C ke 225.40°C. Selain itu, kebolehbasaan turut meningkat dengan peningkatan kuantiti indium. Mikrostruktur pukal aloi pateri menunjukkan saiz butir aloi menurun dan dendrit β -Sn menjadi lebih halus dengan pertambahan indium. Juga diperhatikan bahawa SAL (Cu, Ni)₆Sn₅ dan

Sn-Cu-Ni-In telah terbentuk dengan penambahan indium dari 0.5wt% hingga 2.0wt% Bersama dengan Cu_6Sn_5 . Penambahan indium sebanyak 2.0wt% telah membawa kepada peningkatan kekuatan mekanikal. Merujuk kepada sifat rayapan aloi dengan indium 2.0wt% menunjukkan rintangan rayap paling tinggi yang disebabkan oleh penghalusan mikrostruktur. Penghalusan butir dan pembentukan sal di dalam aloi pateri mengakibatkan halangan kepada pergerakan kehelan. Berdasarkan eksponent tegasan dan tenaga pengaktifan rayapan yang diperolehi, telah dicadangkan bahawa mekanisme ubah bentuk yang dominan bagi pateri SN100C ditambah indium ialah pendakian kehelan pada julat suhu yang dikaji. Penambahan 2.0 wt% indium diperhatikan dapat menggalakkan penghalusan butir dalam pateri SN100C dengan peningkatan pada sifat mekanikal, kebolehbasahan yang lebih baik dan rintangan rayapan yang lebih baik.

**EFFECT OF INDIUM ADDITION ON MICROSTRUCTURE,
WETTABILITY, SHEAR STRENGTH AND CREEP BEHAVIOUR OF
SN100C SOLDER**

ABSTRACT

Due to environmental concern of lead toxicity, the use of lead-free solder has been widely used in electronic packing industries. In finding alternative of lead-free solder to replace the current lead solder, the lead-free solder should have a melting point close to lead solder (183°C), has good wettability, as well as excellent physical and mechanical properties. Among lead-free solders, Sn-Cu alloy is the most compatible to replace the lead solder. However, Sn-Cu solder has a high melting point and wetting angle compared to lead solder. The high melting point caused high soldering temperature, which might expose the sensitive components and substrate to a risk since it cannot withstand high temperature. The aim of this project is to evaluate thermal behaviour, microstructure, wettability, mechanical properties and creep behaviour of SN100C solder (Sn-0.7Cu-0.05Ni-0.01Ge) with addition of indium. The microstructure characteristics, physical and mechanical properties, and creep behaviour of SN100C solder were investigated using optical microscope (OM), scanning electron microscope, differential scanning calorimetry (DSC), and Instron machine. With indium addition from 0wt% to 2.0wt%, the melting temperature was reduced from 229.64 °C to 225.40°C. The wettability of solder alloys improved with increasing amount of indium. Bulk microstructure of solder alloys showed that the grain size of solder decreased, and β -Sn grain became more refined with increasing amount of indium added. It is also observed that (Cu, Ni)₆Sn₅ and Sn-Cu-Ni-In IMC were formed with indium from 0.5 wt% to 2.0 wt.% alongside the Cu₆Sn₅. The addition

of 2.0wt% of indium also led to an improvement of shear strength. In term of creep properties, the alloy with 2.0wt% indium gave the highest creep resistance due to the refinement of microstructure. The refinement and formation of IMCs in the solder alloys can result in impeding the dislocation movement. According to the obtained stress exponent and activation energies, it is proposed that the dominant deformation mechanism in In-added SN100C solder is dislocation climb over the temperature range investigated. The indium addition at 2.0wt% was observed to induce grain refinement of SN100C solder with higher mechanical properties, better wettability behaviour and improved creep resistance.

CHAPTER 1

INTRODUCTION

1.1 Research Background

Tin-lead (Sn-Pb) solders have been widely used in electronic industry due to its combining advantages, such as low melting temperature, economically affordable and excellent wettability. Despite all these advantages, a switch to Pb-free solders to replace the toxic Pb-based solder in the packaging process of electronic device and components are still occurring rapidly. The toxicity of lead has been a focus of many discussion since the 1930s. Various published researches revealed that lead is hazardous, not only to the environments, but also to human health (Cory-slechta *et al.*, 1983, Davies *et al.*, 1976, Wassink, 1989). Driven by these concerns and international legislation, electronic manufacturing companies and researchers have since concentrating their efforts in fabricating lead-free solder to replace the Sn-Pb solder. Indeed, many research groups have been focusing on developing new Pb-free solders (El-Daly *et al.*, 2011, Keller *et al.*, 2011). The new composition solder alloy must comply to these requirements such as; economically affordable material, good wettability, suitable melting temperature, excellent mechanical and electrical properties, high corrosion resistance and non-toxic for human health and environment (Gain *et al.*, 2010).

The solder should be at least comparable to Sn-Pb solder or better. Considering all of the above criteria, thus far, there are only a handful of lead-free solder alternatives that could be appraised. For binary alloys, Sn-Bi, Sn-Cu, and Sn-Ag appear to be the choice. For ternary and quaternary lead-free alloy alternatives, there are Sn-Bi-Ag, Sn-Ag-In, Sn-Ag-Cu, Sn-Bi-Ag-Cu, and Sn-Ag-Sb-Bi (Zhang, 2010). Numerous investigations by consortia, industry alliances, and individual companies

have led the industry to converge on the ternary eutectic Sn-Ag-Cu (SAC) solder alloys as the primary replacement for the lead-bearing solder in reflow solder application. On the other hand, eutectic Sn-Cu is seen to be more preferable in wave solder application (Shangguan, 2005).

In most electronic packaging applications, it is not usually a single high stress event that breaks a solder joint component, instead it is prolonged or repeated load applications that result in creep failure of solder. Creep test in electronic assembly is the physical phenomenon of a time dependent increasing irreversible deformation when a material acts upon the thermal and power cycles during practical service. In addition, electronic devices that have been used in industrial and vehicle products are more commonly loaded into the more severe environments (Hidaka *et al.*, 2009). Since solder alloys have low melting temperature around 180°C to 240°C, the solder joints are prone to creep deformation at both ambient environmental and high temperature conditions. In thermal cycling condition, creep is expected to be the controlling deformation mode in determining the reliability of circuit board assemblies. Because of creep effects, the total strain range during given loading cycle can be a strong function of solder temperature, the loading time per cycle and the applied solder stress. Besides, the solder metallurgical state, including solder composition, aging condition, and grain size could also influence the creep rate of solder alloys. Hence, it is important to understand the creep behaviour of solder joints in the electronic packaging as it can significantly influence the reliability of the electronic devices.

1.2 Problem Statement

Several tin-based lead-free solder alloys such as Sn-Ag, Sn-Cu, Sn-Au, Sn-Ag-Cu, and Sn-Zn have been developed and applied in the electronic packaging industries (Wiese & Wolter, 2004, Tsao, 2011) but none of them meet all the standards of required material properties (e.g., low melting temperature, wettability, and mechanical properties), have good manufacturing, yet affordable. Processing issues and conditions (involving fluxes) are also need to be taken into consideration for the development of proper alloy composition of lead-free solder. Sn-Cu has currently been proposed as most promising substitutes for lead-containing solder for electronic packaging industries especially in wave soldering (Li *et al.*, 2010). This alloy has many benefits compared to Sn-Pb eutectic alloy, it has good manufacturability, good mechanical properties, and stable interfaces with most metallic substrates and surface finishes, as well as nontoxic.

However, fabricating lead-free solder that have properties and melting point, as well as cost effectiveness close to eutectic tin-lead has been a great challenge to researchers. The Sn-Cu solder alloys has higher melting point and wetting angle compared to tin-lead. The higher melting point caused higher soldering temperature. Most of the sensitive components and substrate cannot withstand high temperature and pose a risk to the polymer substrate and the under-fill material. Studies have shown that a potentially and economically affordable approach to improve the properties of Sn-Cu solder alloys is by the addition of small amount of low melting alloying elements such as Ag and In. Recently, Ag and In-containing Sn-Cu alloys have been reported to demonstrate superior performance, at least in its mechanical strength (El-Daly & Hammad 2011, 2012).

Sn-0.7Cu solder has been proposed as one of the most promising substitutes for lead-containing solder wave, dip and iron soldering process with its inexpensive and good electrical conductivity with melting temperature of 227°C. However, the main drawbacks of high melting temperature, insufficient oxidation resistance characteristic and short lifetime under several thermal cycling compared to Sn-Pb solder joints prevent it to be widely used in application of microelectronic packaging industry. Generally, mechanical creep of soldering material occurs more readily when high temperature are involved. At high temperature the mechanical properties of metal are the result of simultaneous process of strain hardening, due to plastic deformation and softening effect of reconvert and recrystallization (Negm *et al.*, 2010). However, knowledge about the creep behaviour of Sn-Cu solder is very important for successful electronic product development. Study shows that creep behaviour of eutectic Sn-Cu alloys solder with small amount of In and Ag addition improved the creep resistance and lifetime of solder (El-Daly & Hammad, 2012).

Therefore, this project focused on various percentage of indium(In) addition to the Sn-Cu solder to investigate the effect on melting behaviour, microstructure of the bulk solder, wettability, shear strength and creep behaviour of Sn–Cu solders alloy.

1.3 Objective

The objectives of this research are as follow:

1. To evaluate the effect of In addition on melting point, wettability and microstructure of SN100C solder.
2. To measure the changes in wettability and microstructure due to In addition would influence the shear strength and creep behaviour of solder joint on Cu substrate.

1.4 Project Overview

In this project, commercial SN100C (Sn-0.7Cu-0.05Ni-0.01Ge) solder alloy was used with addition of indium (0, 0.5, 1.0, 1.5, 2.0 wt%). Lead free solder alloys were prepared via casting and then poured into steel mould. Bulk solder samples were then characterized in terms of composition using XRF, thermal properties of the solder alloys analyzed via Differential Scanning Calorimetry (DSC) and microstructure by using Fe-SEM equipped with EDX. The microstructure of bulk solder and solder joint was characterized using Fe-SEM equipped with EDX for element analysis. Wetting balance test were used to measure the wettability of solder alloys in terms of wetting time and wetting force.

For the mechanical properties, solder samples were reflowed onto Cu substrate at 280°C, the solder joint samples tested for creep test and shear strength using single lap joint samples. Samples were isothermally aged at 150°C in normal air atmosphere for 100h prior to the testing. This is to evaluate the influence of In alloying element to the rate of IMC growth upon thermal exposure. The fracture surface was observed using Fe-SEM and EDX in order to analyze the failure mode of the specimens. In this project, the conventional SN100C has been set as the reference material. The results obtained were compared with SN100C to evaluate the properties of the fabricated solder alloys.

CHAPTER 2

LITERATURE REVIEW

2.1 Introduction

Soldering is a process of joining two or more metals by heating the solder alloys above its melting temperature and flow the molten solder into the joint with or without the aid of a fluxing agent, leading to the formation of metallurgical bonds between the metal and the respective component. Solder materials can be classified into two basic group which is soft and hard solder based on their basic characteristics which is the melting temperature. Soft solders are solder that have melting point lower than 350°C, this type of solders typically contain tin and lead. Some other materials like bismuth, indium and cadmium are also the major components of soft solders. While in case of hard solders, the melting temperature is slightly above 350°C and zinc, gold, copper, etc., are the major components. Based on the composition, solder can also be classified into two groups which is leaded solder and lead-free solder. Figure 2.1 show the evolution of electronic packaging.

From Figure 2.1, solders in microelectronic packaging are practicable to bond with different electrical components to confirm the electric connection and mechanical integration of electric devices (Tunga, 2008). The packaging technology has evolved significantly since then to meet the demands with higher signal speed, smaller package size, increased functionality for a given area and lower cost. To achieve higher I/O (input/ output) connection per package, the peripheral array evolved into an area array package known as Pin Grid Array (PGA) package. The Small Outline Package (SOP) was developed because of the cost benefits it offered. This later evolved into Quad Flat Packs (QFP) which allowed greater I/O connections per package.

All the packages mentioned above are through-hole packages which require hole drilling in the PCB to assemble the packages. Through-hole packages leave large amount of area on the back side of the board unutilized. Surface mount alternatives to these packages were developed in the 1980s. Surface mount packages, also known as Ball Grid Array (BGA) packages, used solder joints instead of pins to assemble the packages on the board. In addition to the increased available board surface area for additional components placement, the solder joints also reduces the electrical parasitics significantly due to their smaller interconnect lengths. BGA packages have smaller form factors compared to through-hole packages. The BGA packages evolved further in the 1990s to Chip Scale Package (CSP). In a CSP, a package size to silicon size with ratio of 1:2 can be achieved.

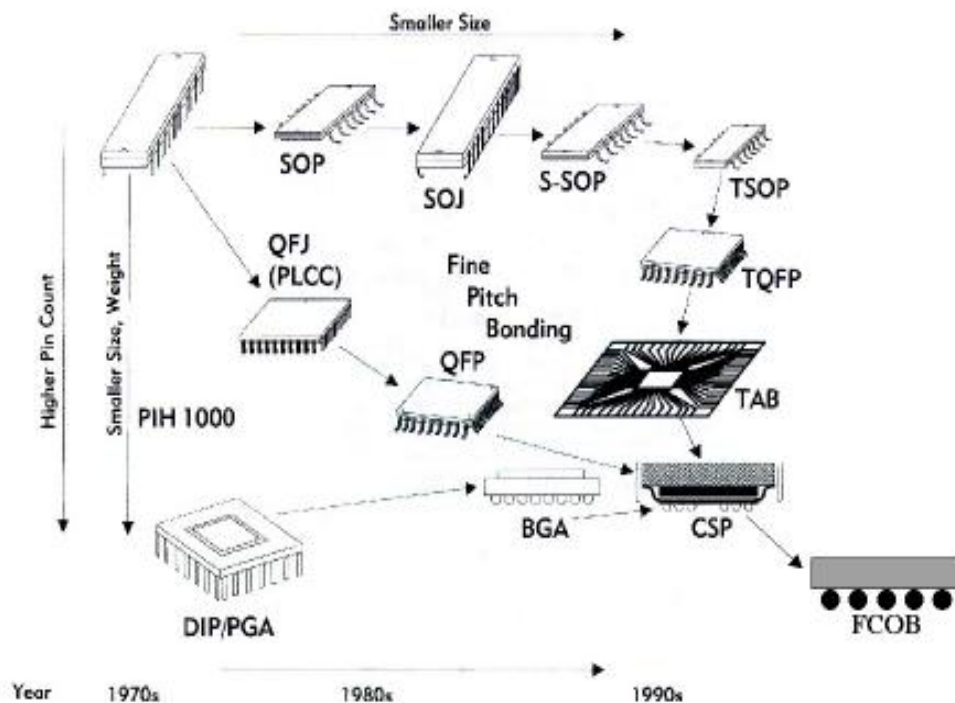


Figure 2.1 Evolution of electronic packaging technology(Tunga, 2008).

2.2 Soldering Technique

Soldering is a metallurgical joining process that used solder as a filler material to join components. Soldering also involved chemical reactions between the solder and bonding surface to be joined which significantly influence the properties and reliability of solder joint later (Ho *et al.*, 2007). Soldering process has some favoured position compared to welding process in term of weldability, type of metals to be joint, amount of heat energy required, etc. A low melting point of filler metal is required to do the joining process without melting down the metal workpieces. There are mainly two types of soldering technologies being used in the industry today to manufacture printed circuit boards (PCB), which are wave soldering and reflow soldering. They are widely used for through-hole and surface mount circuit assemblies. Through-hole soldering refer to the electronic components being soldered via inserts through the holes drilled in the printed circuit board (PCB) while surface mount technology involve mounting or placing the components directly onto the surface of PCB.

2.2.1 Wave soldering

Wave soldering is a large-scale soldering technique in which electronic component are soldered to a PCB to form electronic assembly. The wave soldering process, in principle, consists of three steps i.e. application of flux, pre-heating and the true wave soldering. In the first step, flux was applied on the surface of PCB, the purpose of flux is to improve the wettability of solder and to remove any oxide layer between solder and metal. In the second step, the board was pre-heated where flux is activated and dried, this process also reduces thermal stress placed on PCB in wave soldering step. In the last step, the bottom of the board passes over the molten wave of solder and solder joints are subsequently formed (Jacobson & Humpston, 2005).

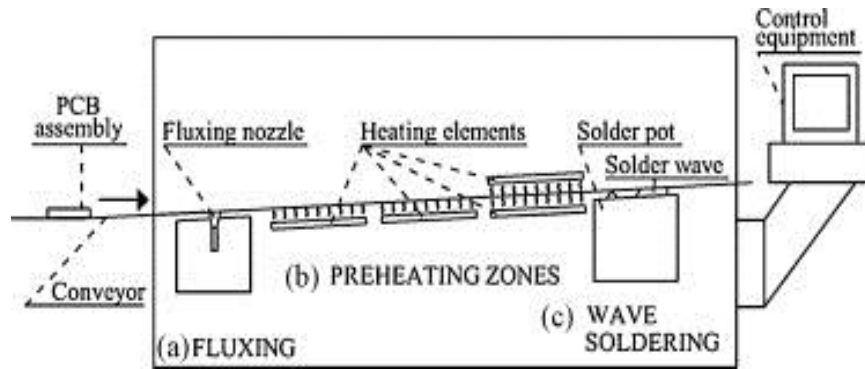


Figure 2.2 Schematic diagram of wave soldering process(Liukkonen et al., 2011).

From Figure 2.2, the wave soldering is divided into three stages, (a) The first stage is where the surface of the PCB assembly is wetted by flux that is pumped through a spray nozzle. Fluxing is performed to improve the wetting of the contact surfaces and to protect the metal. (b) During the next stage, the PCB assembly is preheated usually in multiple heating zones that consist different types of heaters. The purpose of heating is to activate the flux, reduce thermal shock, and to remove possible moisture and impurities at surface. (c) During the last stage, attaching of components is performed by using solder wave. The molten, hot solder is pumped through a narrow slit and the flow touches the surface on the underside of the board, eventually leading to a joint between the lead wires and the board contact surface. In addition, it is common to use smaller and more intensive chip wave to let the solder reach the narrowest spaces between components more easily (Liukkonen *et al.*, 2011).

2.2.2 Reflow Soldering

Reflow soldering is the most common soldering technique of attaching surface mount components to circuit board. In this process, a solder paste containing small solder spheres, flux and solvent is applied on surface of board before placing the

surface mount components. The solder paste acts as temporary glue that hold the components in place prior to the soldering process. The board is heated above the melting temperature of solder. At this point, the flux activated removed the oxide layer and solder joint was subsequently formed (Shangguan, 2005).

Adequate reflow temperature is needed for the solder to melt, flow and wet, interact with the copper on the pad and the component termination, and form good intermetallic bond when cooled and solidified. Typically, temperature for reflow process is 30°C above the melting temperature is desired. For lead-free soldering, because of the concerns about the thermal stability of the components, efforts are needed to minimise the soldering temperature. For SAC alloy with the eutectic temperature at 217°C, the minimum reflow peak temperature should be 235°C for large volume manufacturing, considering process robustness, yield, variety of component finishes, oven thermal stability and tolerance. The dwell time or time above liquidus (TAL) is typically 40-90s (Suhir *et al.*, 2007).

In the reflow process, the high melting points of the typical Pb-free Sn-based solders requires reflow to occur above 240°C. The recommended reflow profile temperature should be above 240°C and with varying product, size and mass. Usually Sn-Pb solders that commonly have peak reflow temperature of 215-245°C with 20-60 seconds above Sn-Pb melting temperature which is 183°C. While compared with the typical reflow temperature range for Pb-free (Sn-Ag) solder is 240-250°C with 40-80 seconds, if over the limit it may damage the component, burn and harden the flux. By rising the temperature, it enables alloying element such as Sn, Bi, Zn, Ag, In, and Cu diffusing from the substrate to acquire more energy, intensifying the orbital interaction among these atoms. The solder spreads on the Cu substrate in the first place and then

an element that separates away from the Cu substrate forms at the interface (Clara 2006). Figure 2.3 shows the reflow soldering process.

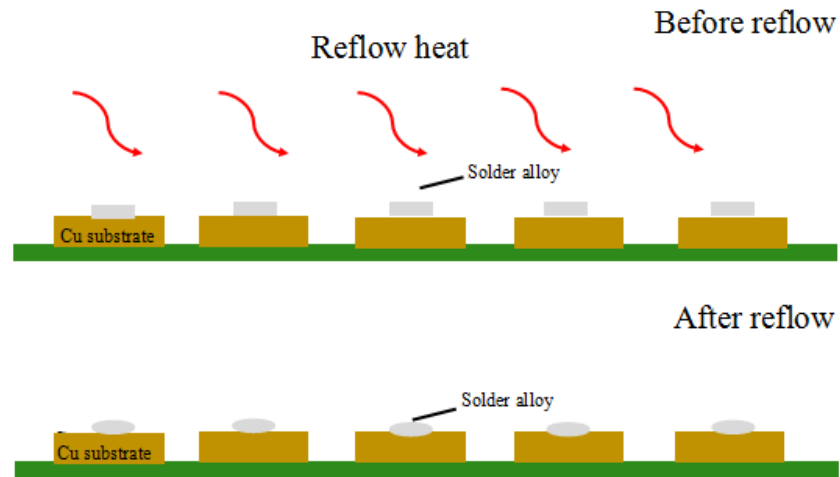


Figure 2.3 Schematic diagram of reflow soldering process (Ressana,2016).

2.2.3 Hand Soldering

Hand soldering is the basic method process involved by applying heat with the combination of solder and flux to produce joint formation. This process is typically performed with soldering iron, soldering gun or torch, or occasionally a hot-air pencil. Compared with conventional method, this manual process required a certain extent skill and experience (Jacobson & Humpston, 2005, Wassink, 1989).

Hand soldering is nothing but a soldering operation that can be performed by hand using tools. It is done during PCB rework in a production unit when a PCB gets rejected or failed to pass the quality test. Soldering quality and performance depend on board thickness, temperature, flux type and techniques. With proper tools and techniques board, rework productivity would increase while damaged to PCB will be

kept at minimum. Hand soldering is also done while repairing and reworking on printed circuit boards.

Hand soldering need a good quality soldering iron or temperature controlled soldering station that run on electricity. If you are dealing with ESD-sensitive PCB and electronic components, then you need an ESD-safe soldering station. If you are doing lead-free soldering, you will probably need a temperature-controlled soldering iron or soldering station with higher wattage because the melting point of lead-free solder is higher than tin-lead solder. Figure 2.4 shows the hand soldering technique. When iron's tip touches a lead, heat is conducted into the joint, causing the heating element to power up to replace the heat loss. When the tip is removed from the joint, heat energy continues to flow instantly, as if the mass of the joint were still present.

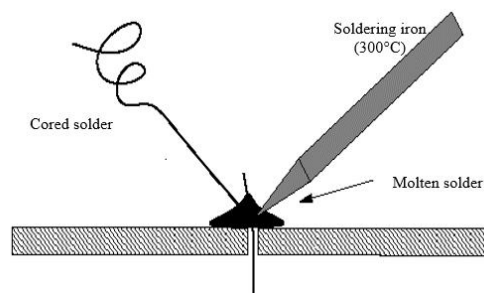


Figure 2.4 Schematic diagram of hand soldering process (Clear, 2011).

2.3 Flux

The key to good solderability lies in ensuring that the surface to be joined is clean. The surface of solder joint must maintain its cleanliness so that metallic continuity at the interface can be achieved during soldering. The cleaning process is called fluxing and the material used is flux. Flux is a substance used to promote fusion

between solder and substance. Flux function as a chemical to remove oxides from the surface as well as from the solder surface, providing a barrier against further oxidation of surface, facilitating heat transfer into the joint surface and acting as medium for metal ion transfer as part of the wetting process (Wassink, 1989).

These functions are important in soldering process in order to achieve proper wetting of solder on substrate to form the joint. The type of flux must be carefully chosen according to the melting point of solder itself (different solder alloys elements need different kind of fluxes). A good flux should melt at a temperature around 20°C to 50°C lower than the melting point of solder. There are various fluxes available for many purpose and application. Flux can be categorised by three different types that are resin flux, water soluble flux and no clean flux. Each type of flux is suited for specific types of assemblies. To improve wetting properties, development of the flux chemistry is the key issue (Berglund, 2003).

2.4 Lead Free Solder

In electronic industry, transition from lead-tin solder to lead-free solder is mainly due to health and environmental concerns. The material science community such as researchers and manufactures has been developing new alternatives to replace the Sn-Pb solders. There are many solders that are currently available in the market but does not fulfil the required properties, thus researches are still being conducted to seek solutions for this issue. Generally, selection of lead-free solder alloys is based on few properties such as melting temperature, solderability, electrical conductivity, mechanical properties, microstructural characteristics, toxicity, cost and availability.

Several lead-free solder alloys have been developed from binary and ternary alloys system, most of lead-free solder alloys are based on Sn as the base alloy.

2.4.1 Binary Alloy

2.4.1.1 Tin – Copper (Sn-Cu) Solder Alloy

The eutectic Sn–0.7Cu shows same level of performance as eutectic Sn–Pb. As reported by (Satyanarayan & Prabhu, 2011), Sn–0.7Cu is found to be less toxic as compared to Sn–5Bi–5Ag, Sn–2Ag, Sn–3.5Ag, Sn–3.2Ag–0.5Cu and Sn–5Sb solder alloys. Sn–0.7Cu solder alloy is used as alternative to lead-based solder alloy due to its excellent physical and mechanical characteristics. It is also lower in cost compared to other lead-free solders. Thus, making it preferable for soldering in electronic applications.

The solid solubility of copper in tin at eutectic temperature is only 0.006 wt.% or 0.01 wt.% and the intermediate phase corresponds to 44.8 to 46% Sn. The solder is composed of large, Sn rich grains with a fine dispersion of Cu_6Sn_5 intermetallic. According to the phase diagram in Figure 2.5, the stable intermetallic phases below 300°C are ϵ and η phases. The ϵ phase has a composition close to Cu_3Sn and corresponding η has the composition of Cu_6Sn_5 .

The binary alloy of Sn–Cu has a eutectic composition of Sn–0.7Cu (wt.%) and a eutectic temperature of 227°C. A hypoeutectic Sn–Cu solder microstructure composed of primary β -Sn dendrites and grey eutectic colonies. If Sn–0.7Cu alloy is under low temperature, it will follow the equilibrium solidification path, $L \rightarrow \beta\text{-Sn} + \text{Cu}_6\text{Sn}_5$, with Cu precipitating as hollow rods of Cu_6Sn_5 . (Kotadia *et al.*, 2014) reported during reflow, the large Sn-rich dendrites interspersed with fine Cu_6Sn_5

intermetallic at solder matrix. At the solder/substrate interface, it was reported that through the diffusion of Cu atom from Cu substrate with Sn atom that forms a thin layer of Cu_3Sn and a thick scallop layer of Cu_6Sn_5 . At the eutectic temperature, the solid solubility of Cu in Sn is only 0.006–0.01 wt.%, with the intermediate phase corresponding to 44.8–46% Sn.

Recently, there are limited data available on the microstructure and mechanical characteristics of Sn-Cu solder alloys. (Satyanarayan & Prabhu, 2011). The Sn–0.7Cu alloy is suitable for high temperature applications like automotive industry. It has shown a significant improvement in creep/fatigue data over Sn–Pb alloys. It is also used in surface mount technology (SMT), plated through hole, ball grid arrays and flip chip technology. In this study, Sn–0.7Cu solder alloy system was chosen to lower the cost of the alloy (i.e., instead of using Au and Ag). To enhance the solder properties of this alloy by adding Ni and In into Sn.0.7Cu and see how it would improve the properties of the alloy.

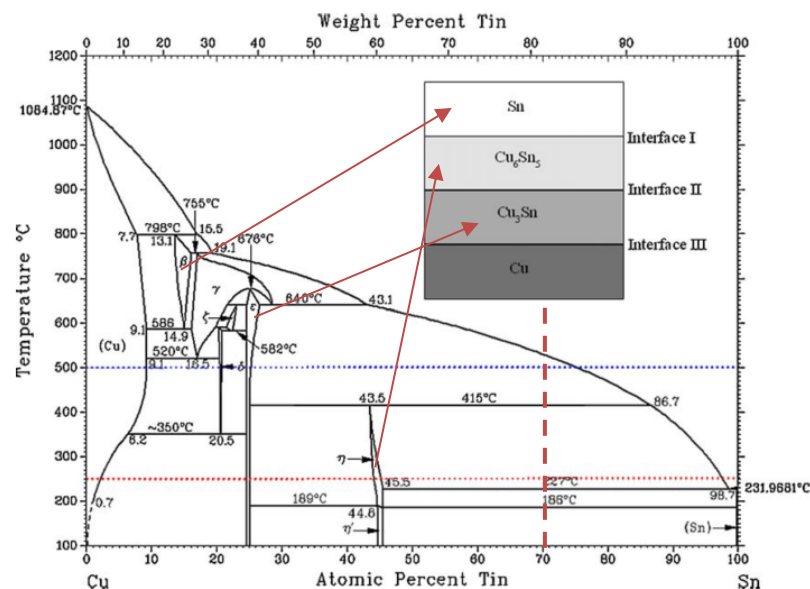


Figure 2.5 Sn-Cu phase diagram (Satyanarayan & Prabhu, 2011).

2.4.1.2 Tin – Silver (Sn-Ag) Solder Alloy

The Sn-Ag solder alloy has been widely used in electronic industry application because it has better mechanical properties compared to Sn-Pb eutectic solder alloy. Figure 2.6 shows Sn-Ag binary alloy phase diagram that can be used to understand melting behaviour. Sn-Ag binary phase diagram Ag_3Sn when the temperature is the eutectic temperature $221^\circ C$ or lower. The soldering process of Sn-Ag/Cu consist of heat up, heat preservation and cooling. In the two-former stage, base Cu is consumed which results in the increase of Cu concentration in the liquid solder. Sn is also consumed, which give rise to the concentration of Ag in the local area near the interface. As the concentration of Ag reached a certain value, Ag will separate out in the form of Ag_3Sn IMC. Meanwhile, along with the temperature decrease, the solubility of Ag in liquid solder also decrease, which results in the precipitate of Ag_3Sn in cooling process inside the solder.

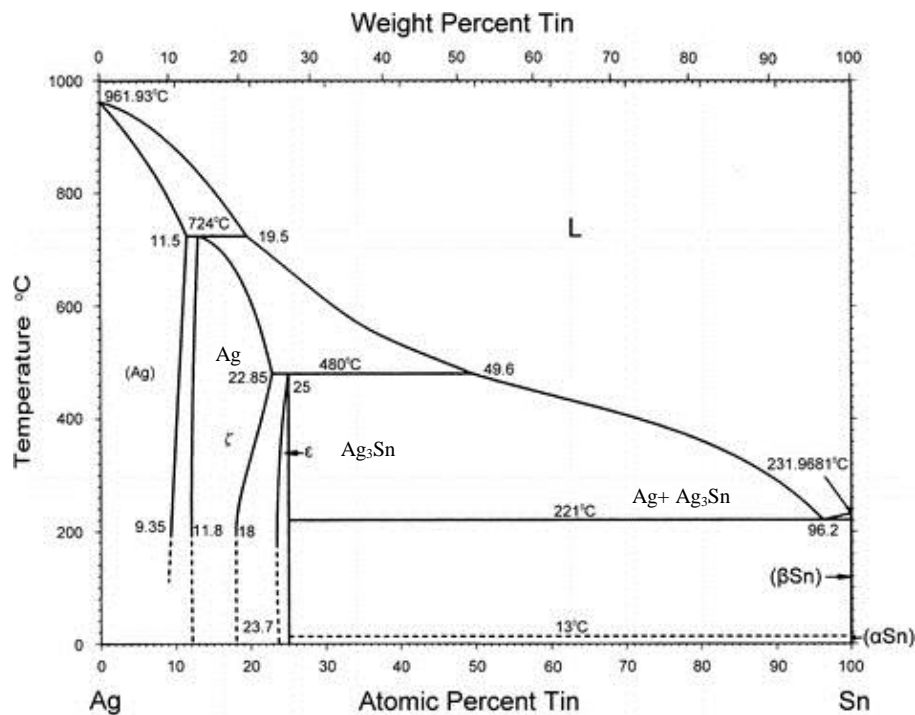


Figure 2.6 Phase diagram of Sn-Ag solder alloys.

2.4.1.3 Tin – Indium (Sn-In) Solder Alloy

As shown in the Figure 2.7, the Sn-In solder alloy has a eutectic point at 49 at% Sn and melting temperature around 120°C. Due to its low melting temperature, soft solder alloy, ductility, low tensile strength and excellent wetting properties, Sn-In solder alloy is suitable for low temperature solders alloy. On the other hand, compound InSn_4 will not form due to solubility limit of indium in Sn is about 7.0wt%, high amount of indium (more than 7.0wt%) in Sn-solder base are not recommended for reflow or wave soldering due to its extreme softness (Wassink, 1989). Furthermore, it is not economically practical for Sn-In to replace Sn-Pb solder because In has higher manufacturing cost (Puttlitz & Stalter, 2004).

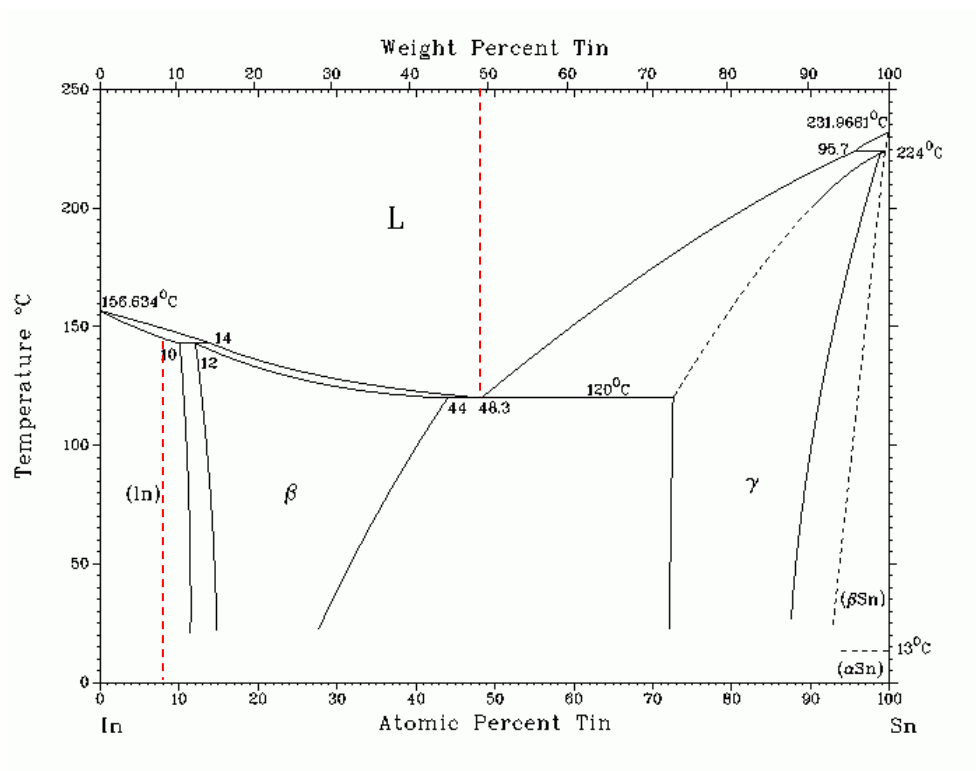


Figure 2.7 Phase diagram of Sn-In solder alloys (www.Himikatus.ru, 2017).

2.4.2 Ternary Alloys

2.4.2.1 Tin-Silver-Copper (Sn-Ag-Cu) solder alloy

The Sn-Ag-Cu solder alloys have been developed as promising lead-free solder for Sn-Pb solder replacement. The addition of Cu in range 0.3 to 0.7 wt% into Sn-Ag solder alloy resulted in ternary solder alloy with low melting temperature, ranges from 216°C to 220°C, depending on composition of the element. Based on the Sn-Ag-Cu ternary phase diagram shown in Figure 2.8, the ternary composition is at Sn-3.8Ag-0.7Cu with melting temperature 217°C. The increasing amount of Ag will increase the melting temperature of solder alloy. The formation of intermetallic compounds between primary element Sn either with Ag or Cu in SAC alloy affects the properties of alloys. A ternary eutectic composition of SAC consists of 95.46 wt% Sn, 3.58 wt% Ag and 0.96 wt% Cu.

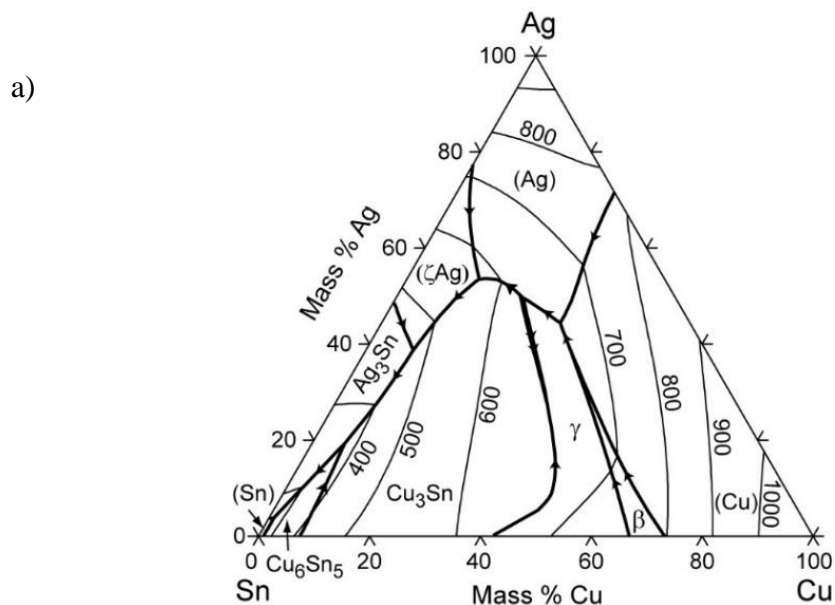


Figure 2.8 (a) Ternary phase diagram showing the Sn–Ag–Cu ternary eutectic reaction and (b) Calculated liquidus surface for Sn–Ag–Cu (Kattner & Boettinger, 1994) (cont.)

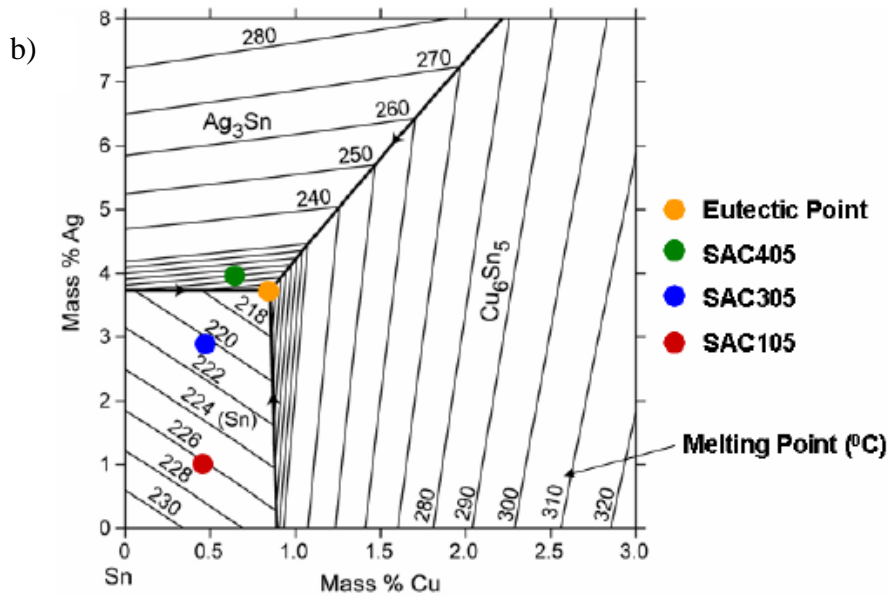


Figure 2.8 (a) Ternary phase diagram showing the Sn–Ag–Cu ternary eutectic reaction and (b) Calculated liquidus surface for Sn–Ag–Cu (Kattner & Boettinger, 1994) (cont.)

2.4.2.2 Tin-Copper-Zinc (Sn-Cu-Zn) Solder Alloy

Sn-Cu-Zn alloys have recently received considerable interest as negative electrodes, corrosion resistant layer and candidates for lead-free solder (Ali *et al.*, 2016). Figure 2.9 shows the Sn-Cu-Zn ternary phase diagram. The phase diagram showed that there were Cu-Sn and Cu-Zn binary compound, but no ternary compound has been found. The addition of Zn in Sn-Cu solder reduced the melting point as well as its cost (El-Daly & El-Taher, 2013). Since Zn is highly reactive metal, Zn that is exposed to air is readily oxidizes in the liquid state of Sn-Cu-Zn solder. Therefore, only small amount of Zn is needed to cause formation of oxide layer at solder interface (Karl, 2004). Other than that, addition of Zinc can increase the shear strength of the solder alloy (Luo *et al.*, 2013).

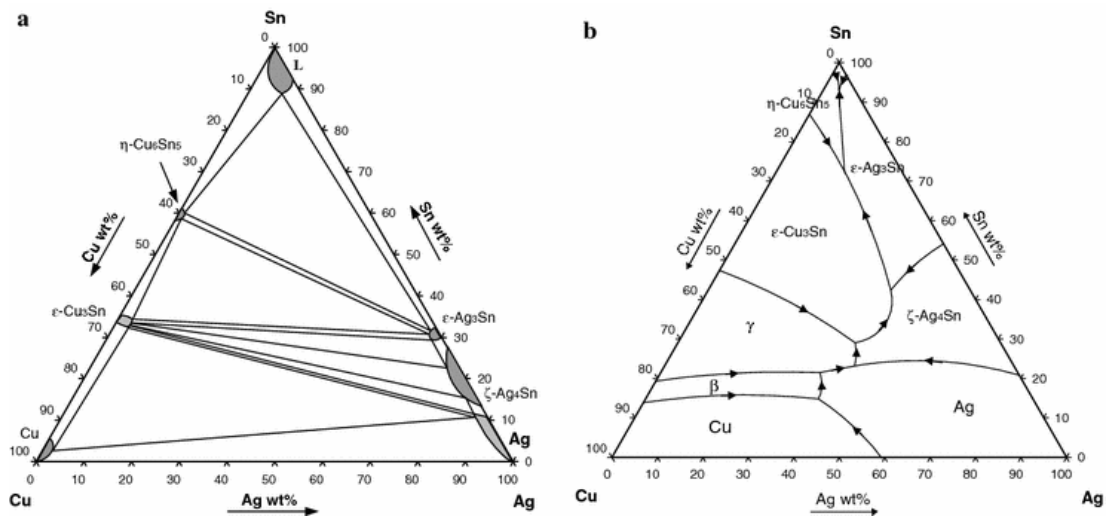


Figure 2.9 Ternary phase diagram showing the Sn-Cu-Zn ternary, and (b) Calculated liquidus surface for Sn-Cu-Zn (Ali et al., 2016).

2.4.3 Effect of Indium Addition on Sn Based Lead-Free Solder

One of the main reasons of adding Indium into Sn based lead free solder is its effectiveness in lowering the melting point. Addition of Indium in lead free solder alloy will lead to significant reduction of melting point and pasty range of solder alloy. Report showed that an increase of In content in Sn-0.7Cu will lead to a decrease in eutectic melting temperature of alloy from 229°C to 224°C, as In content increased from 0.1 to 2wt% (El-Daly and Hammad, 2012). The decrease in the melting point of the alloy solders could be possibly attributed to an increase of the surface instability and the variation in physical properties of the grain boundary/interfacial characteristics rendered by the reinforcing IMCs phases (El-Daly and Hammad, 2012). Besides temperature, pasty range of solder alloy also decreased with the addition of In, which is lower than that of the pasty range of Sn-Pb solder with 11.5°C. This improvement is

crucial as large pasty range in solder alloy may cause problem in manufacturing (El-Daly and Hammad, 2012).

Addition of 0.3wt% In in Sn-0.7Cu-0.2Ni solder alloy has also been reported to lower the hardness of solder alloy. The lowering in hardness is due to the formation of new Indium containing alloy phase. In general, the addition of In refined the microstructure. With the increase of In content in solder alloy, the IMCs formed become coarser, which lead to the decrease in hardness of solder alloy (Li *et al.*, 2014). The decrease in hardness of solder alloy with increasing In content can also be related to the inhomogeneity of the system (Negm *et al.*, 2010) (Wang *et al.*, 2013). However, it is reported that the microhardness of Sn-9Zn solder alloy increased with the amount of In. The increase in In content caused a change in the length of Zn rich phases and also a decrease in the amount of Zn rich phase. The increase in size of Zn rich phases contributes to the enhancement of the overall strength and hardness of solder alloy (Wang *et al.*, 2013). In term of creep resistance, addition of In shows better creep resistance compared to Sn-Cu solder alloy. This was attributed to the formation of the γSnIn_4 IMCs that impede the dislocation movement and reinforced the solder matrix (El-Daly and Hammad, 2012).

In addition, adding In in Sn-0.7Cu-0.2Ni solder alloy improved wettability of the solder alloy. Improved wettability of In containing solder alloy give lower wetting angle and wider spreading area on substrate, which is 15.6% wider than Sn-Cu lead free solder. The In containing alloy was found to give better wettability on both copper and nickel substrate (Li *et al.*, 2014). Addition of In in Sn-0.7Cu-0.2Ni solder alloy also improved the corrosion resistance of solder alloy. This is due to the formation of dense corrosion product that will later deposited on the surface of solder joint and slow down the corrosion on solder surface (Li *et al.*, 2014).

The effect of In addition on the microstructure of solder alloy showed the formation of γSnIn_4 IMCs that reinforced solder matrix and suppressed the formation of large $\beta\text{-Sn}$ dendrite cell and instead favours the formation of eutectic regions on the surface of $\beta\text{-Sn}$ matrix due to the presence of γSnIn_4 IMCs (El-Daly and Hammad, 2012). The thickness of IMC form was found to increase with the addition of In (Li *et al.*, 2014).

There were also reports that indicated In shows strong segregation behaviour to liquid, which can result into a high concentration of In in the melt. If In concentration in the solder is high enough, more than 16 atomic percentage (at%), the segregation behaviour was seen to result into strong coring (Korhonen and Kivilahti, 1998, Laurila *et al.*, 2010).

2.5 Solder Characterization

Solderability can be defined simply as “the ability of a surface to be wet by molten solder”. Wettability of a liquid on solid could be characterised in term of degree of wetting and rate of wetting. Degree of wetting is indicated by the contact angle between liquid and solid, known as wetting angle, while the rate of wetting is indicated by wetting time. There are many tests to evaluate the wetting properties of liquid and solid and the common test that provide the most reliable data is spreading test and wetting balance (Satyanarayan & Prabhu, 2012).

2.5.1 Wettability (Spreading test)

Wetting is the ability of a liquid to maintain contact with solid surface, resulting from intermolecular interaction when the two metals are brought together. The

wettability of solder on the surface is an important aspect for solderability classification. Its ability is to create uninterrupted layer of soldering material on surface when they are in contact. To create a good joint, it is necessary to reach good wettability on contact substrate. The wetting angle is affected by number of factors including surface roughness, time, flux being used and flux effectiveness and temperature (Ramani, 2017). The contact angle is the result of surface tension between solid and liquid (molten solder) as shown in Figure 2.10.

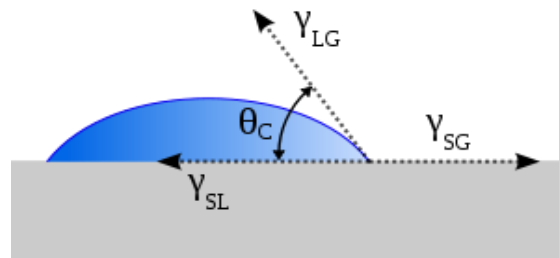


Figure 2.10 Schematic diagram of wetting angle using Young-Dupre equation (Ayyad 2010).

Table 2.1 Wetting categories of solder alloys (Mayhew and Wicks, 1971).

Categories	Ranges
Excellent	$0^{\circ} \leq \theta < 20^{\circ}$
Very good	$20^{\circ} \leq \theta < 30^{\circ}$
Good	$30^{\circ} \leq \theta < 40^{\circ}$
Adequate	$40^{\circ} \leq \theta < 55^{\circ}$
Poor	$55^{\circ} \leq \theta < 70^{\circ}$
Very good	$70^{\circ} \leq \theta < 90^{\circ}$

Wettability studies also usually involve the measurement of contact angles as the primary data, which indicates the degree of wetting when a solid and liquid interacts. Small contact angles ($\ll 90^\circ$) correspond to high wettability, while large contact angles ($\gg 90^\circ$) correspond to low wettability. Young's equation is used to determine the contact angle between solder and the substrates, and the balance of surface tension at the interface (Equation 2.1) (Zhang *et al.*, 2009). Table 2.1 shows the wetting categories of solder alloys.

The theoretical contact from consideration of thermodynamic equilibrium between three phases. The liquid phase of droplet (L), the solid phases of the substrate (S) and gas phase of ambient (G). Three parameters that influence the shape of liquid drop at solid surface are; γ_{SL} , the surface tension between solid and liquid; γ_{LG} , the surface tension between solid and gas and; γ_{SG} , the surface tension between solid and gas. These three parameters are linked with the contact angle (Θ) by Young's equation as shown in Equation 2.1. at equilibrium, the chemical potential in three phases should be equal:

$$\gamma_{SL} + \gamma_{LG} \cos \theta - \gamma_{SG} = 0 \quad \text{Equation 2.1}$$

$$\cos \Theta = \frac{\gamma_{SG} - \gamma_{SL}}{\gamma_{LG}} \quad \text{Equation 2.2}$$

When good wetting occurs, the contact angle should be small (i.e γ_{SL} and γ_{LG} smaller and γ_{SG} larger). The term γ_{SG} can be minimised by cleaning the surface of the substrate. The presence of absorbing material such as water vapor, dust and other non-metallic surface films on substance can reduce the γ_{SG} and increase the contact angle. Therefore, it is important for solder joint surface to be clean and has suitable flux or protective atmosphere to achieve good wetting angle.